Parity doubling structure of nucleon at non-zero density in the holographic mean field theory

Bing-Ran He[1]

Department of Physics, Nagoya University, Nagoya 464-8602, Japan

Abstract

We develope the holographic mean field approach in a bottom-up holographic QCD model including baryons and scalar mesons in addition to vector mesons and pions. We study the effect of parity doubling structure of baryons at non-zero density to the equation of state between the chemical potential and the baryon number density. The result shows that the effective mass decreases with increasing density, and that the rate of decreasing is more rapid for larger percentage of the mass from the chiral symmetry breaking.

1 Introduction

The spontaneous chiral symmetry breaking (χSB) is one of the most important features in low-energy QCD. This is considered to be the origin of several hadron masses, such as the lightest nucleon mass. However, there is a possibility that only a part of the lightest nucleon mass is generated by the spontaneous χSB and the remaining part is the chiral invariant mass. This structure is nicely expressed in so called parity doublet models.

It is an interesting question to ask how much amount of the nucleon mass is generated by the spontaneous χSB, or to investigate the origin of nucleon mass. Studying dense baryonic matter would give some clues to understand the origin of our mass, since a partial restoration of chiral symmetry will occur at high density region. We expect that the mass generated by the spontaneous χSB will become small near the chiral phase transition point.

2 Parity doubling structure of the model

2.1 model

The fields relevant to the present analysis are the scalar meson field X and two baryon fields N_1 and N_2, as well as the 5-dimensional gauge fields R_A and L_A. The bulk action is given as

$$S = S_{N_1} + S_{N_2} + S_{\text{int}} + S_X , \tag{1}$$

where

$$S_{N_1} = \int \mathrm{d}^5x \sqrt{g} \left\{ \frac{i}{2} \bar{N}_1 e_A^M \Gamma^A \nabla_M N_1 - \frac{i}{2} \left(\nabla_M^\dagger \bar{N}_1 \right) e_A^M \Gamma^A N_1 - M_5 \bar{N}_1 N_1 \right\} , \tag{2}$$

$$S_{N_2} = \int \mathrm{d}^5x \sqrt{g} \left\{ \frac{i}{2} \bar{N}_2 e_A^M \Gamma^A \nabla_M N_2 - \frac{i}{2} \left(\nabla_M^\dagger \bar{N}_2 \right) e_A^M \Gamma^A N_2 + M_5 \bar{N}_2 N_2 \right\} , \tag{3}$$

$$S_{\text{int}} = -\int \mathrm{d}^5x \sqrt{g} G \left\{ \bar{N}_2 X N_1 + \bar{N}_1 X^\dagger N_2 \right\} , \tag{4}$$

$$S_X = \int \mathrm{d}^5x \sqrt{g} \, \mathrm{Tr} \left\{ |DX|^2 - m_5^2 |X|^2 - \frac{1}{4g_5^2}(F_L^2 + F_R^2) \right\} , \tag{5}$$

with $M_5 = 5/2$ and $m_5^2 = -3$ being the bulk masses for baryons and mesons, G the scalar-baryon coupling constant, g_5 the gauge coupling constant. The vielbein e_M^A appearing in Eqs. (2) and (3)

---

[1]e-mail address: `he@hken.phys.nagoya-u.ac.jp`

satisfies $g_{MN} = e_M^A e_N^B \eta_{AB} = \frac{1}{z^2}\text{diag}(+---)$, where M labels the general space-time coordinate and A labels the local Lorentz space-time, with $A, M \in (0,1,2,3,z)$. By fixing the gauge for the Lorentz transformation, we take the vielbein as $e_M^A = \frac{1}{z}\eta_M^A = \frac{1}{z}\text{diag}(+----)$. The Dirac matrices Γ^A are defined as $\Gamma^\mu = \gamma^\mu$ and $\Gamma^z = -i\gamma^5$ which satisfy the anti-commutation relation $\{\Gamma^A, \Gamma^B\} = 2\eta^{AB}$. The covariant derivatives for baryon and scalar meson are defined as

$$\nabla_M N_1 = (\partial_M + \frac{i}{4}\omega_M^{AB}\Gamma_{AB} - i(A_L^a)_M t^a)N_1, \tag{6}$$

$$\nabla_M N_2 = (\partial_M + \frac{i}{4}\omega_M^{AB}\Gamma_{AB} - i(A_R^a)_M t^a)N_2, \tag{7}$$

$$D_M X = \partial_M X - iA_{LM}X + iXA_{RM}, \tag{8}$$

where $\Gamma^{AB} = [\Gamma^A, \Gamma^B]/(2i)$. ω_M^{AB} is the spin connection given by $\omega_M^{AB} = \frac{1}{z}(\eta^A_Z\eta^B_M - \eta^A_M\eta^B_Z)\eta^{ZZ}$.

2.2   parity doubling structure

The solution for scalar field X is obtained as[4;5] $X_0(z) = \frac{1}{2}Mz + \frac{1}{2}\sigma z^3$, where M is the current quark mass and σ is the quark condensate $\langle\bar{q}q\rangle$.

We decompose the bulk fields N_1 and N_2 as $N_1 = N_{1L} + N_{1R}$, $N_2 = N_{2L} + N_{2R}$, where $N_{1L} = i\Gamma^z N_{1L}$, $N_{1R} = -i\Gamma^z N_{1R}$, $N_{2L} = i\Gamma^z N_{2L}$, $N_{2R} = -i\Gamma^z N_{2R}$. The mode expansions of $N_{1L,R}$ and $N_{2L,R}$ are performed as

$$N_{1L,R}(x,z) = \sum_n \int \frac{d^4p}{(2\pi)^4}e^{-ipx}f_{1L,R}^{(n)}(z)\psi_{L,R}^{(n)}(p),$$

$$N_{2L,R}(x,z) = \sum_n \int \frac{d^4p}{(2\pi)^4}e^{-ipx}f_{2L,R}^{(n)}(z)\psi_{L,R}^{(n)}(p). \tag{9}$$

It is convenient to introduce $f_+^{(n)}$ as $f_{+1}^{(n)} = f_{1L}^{(n)} + f_{2R}^{(n)}$, $f_{+2}^{(n)} = f_{1R}^{(n)} - f_{2L}^{(n)}$, which satisfy

$$\partial_z f_{+1}^{(n)} = \frac{2 + M_5}{z}f_{+1}^{(n)} - \frac{1}{2}G\sigma z^2 f_{+2}^{(n)} - m_+^{(n)}f_{+2}^{(n)},$$

$$\partial_z f_{+2}^{(n)} = \frac{2 - M_5}{z}f_{+2}^{(n)} - \frac{1}{2}G\sigma z^2 f_{+1}^{(n)} + m_+^{(n)}f_{+1}^{(n)}, \tag{10}$$

with $m_\pm^{(n)}$ corresponding to mass eigenvalues.

For solving Eq. (10) we use the boundary conditions for $f_{+1}^{(n)}$ and $f_{+2}^{(n)}$ as Tab 1:

	UV	IR
$f_{+1}^{(n)}$	0	1
$f_{+2}^{(n)}$	0	c_1

Table 1: Boundary condition when using shooting method.

For a given value of c_1, we first adjust the coupling G to ensure that the lowest eigenvalue becomes the nucleon mass of $0.94\,\text{GeV}$. We show how the value of G changes depending on the value of c_1 in Fig. 1.

We next calculate the masses of higher excited nucleons using the value of G determined above for fixed c_1. We show the c_1-dependence of several masses in Fig. 2. Here, $N(+)$ denotes the states with positive parity while $N(-)$ stands for negative parity. This figure shows that, for $c_1 > c_1^* \approx 0.12$, the first excited state carries the negative parity and the second the positive parity, and so on. For $c_1 < c_1^*$, on the other hand, the first excited state is the positive-parity excited nucleon, which seems consistent with the experimental data.
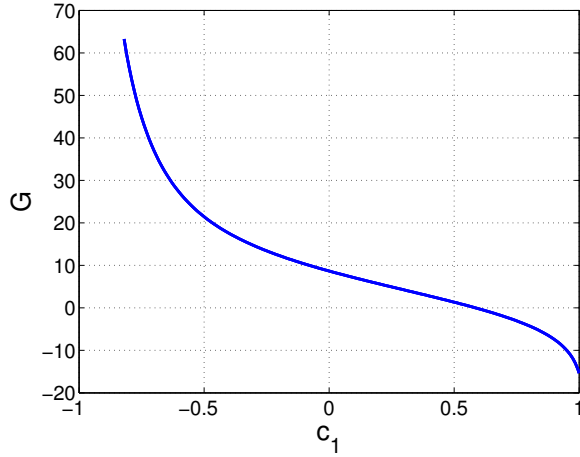
Figure 1: Value of G determined from c_1 to make the lowest eigenvalue to be the nucleon mass of $0.94\,\mathrm{GeV}$.
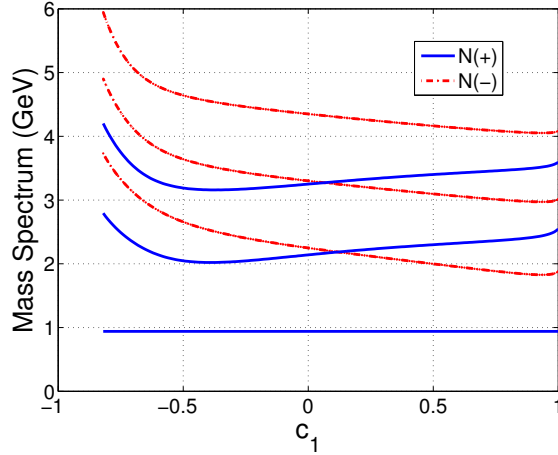

Figure 2: c_1 dependence of excited nucleon masses.

For understanding the meaning of c_1, we investigate the effect of dynamical chiral symmetry breaking on the nucleon mass. For quantifying this effect, we take $\sigma = 0$ and calculate the mass eigenvalue by solving

$$
\begin{aligned}
\partial_z f_{+1}^{(n)} &= \frac{2 + M_5}{z} f_{+1}^{(n)} - m_0^{(n)} f_{+2}^{(n)}, \\
\partial_z f_{+2}^{(n)} &= \frac{2 - M_5}{z} f_{+2}^{(n)} + m_0^{(n)} f_{+1}^{(n)},
\end{aligned}
\tag{11}
$$

for several choices of c_1. We consider the lowest eigenvalue $m_0^{(1)}$, denoted as just m_0, as the chiral invariant mass of nucleon. In Fig. 3, we plot the c_1 dependence of the value of $1 - m_0/m_N \equiv \frac{m(\bar{q}q)}{m_N}$ which shows the percentage of the nucleon mass coming from the spontaneous chiral symmetry breaking. From Fig. 3 we conclude that, in the case of $c_1 = 0$, which is chosen in Ref. [3], all the nucleon mass comes from the spontaneous chiral symmetry breaking. On the other hand, when $c_1 > 0.25$, more than half of the nucleon mass is the chiral invariant mass.
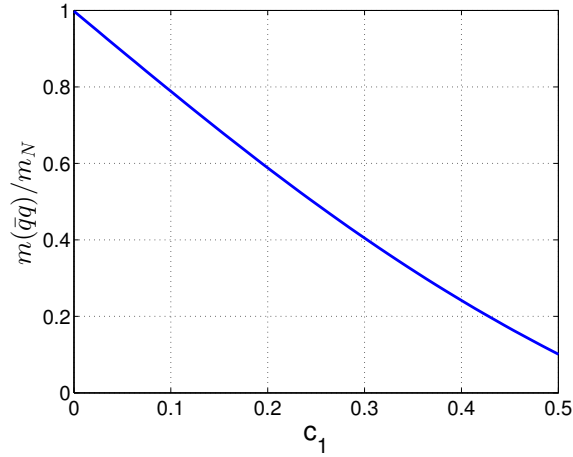
Figure 3: c_1-dependence of $\dfrac{m(\bar{q}q)}{m_N}$, which shows the percentage of the nucleon mass coming from the spontaneous chiral symmetry breaking.

3   Equation of state in the holographic mean field approach to the model

In the holographic mean field theory, all the 5D fields are decomposed into the mean fields which depend only on the 5th coordinate z and the fluctuation fields. In the present analysis, we consider the symmetric nuclear matter, so that the proton and the neutron have the same mean fields. Furthermore, we assume that the mean fields for the vector and axial-vector gauge fields except the $U(1)_V$ gauge field and the traceless part of the scalar field are zero. The equations of motion for the mean fields can be simplified as[8],

$$
\begin{aligned}
\partial_z^2 X &= \frac{3}{z}\partial_z X + \frac{m_5^2}{z^2}X + \frac{G}{2z^2}(N_+^\dagger N_+ - N_-^\dagger N_-)\,, \\
\partial_z^2 V_0 &= \frac{1}{z}\partial_z V_0 + \frac{g_5^2}{z^3}(N_+^\dagger N_+ + N_-^\dagger N_-)\,, \\
\partial_z N_+ &= \frac{2+M_5}{z}N_+ - \frac{1}{z}GXN_- - V_0 N_-\,, \\
\partial_z N_- &= \frac{2-M_5}{z}N_- - \frac{1}{z}GXN_+ + V_0 N_+\,.
\end{aligned}
\tag{12}
$$

We change the IR values of N_+ and N_- to control the baryon number density, which is written in terms of the baryon fields as

$$
\rho_{\mathrm{b}} = \int \frac{dz}{2z^4}(N_+^\dagger N_+ + N_-^\dagger N_-) = \int dz\,\rho(z)\,.
\tag{13}
$$

The boundary conditions at finite density is shown in Table 2.

We first study the density dependence of the chiral condensate for checking the partial chiral restoration. Here we define the in-medium condensate through the holographic mean field $X(z)$ as $\sigma = \left.\frac{2X(z)}{z^3}\right|_{z=z_{\mathrm{UV}}}$. We plot the density dependence of the σ normalized by the vacuum value σ_0 in Fig. 4. This shows that the quark condensate σ decreases with the increasing number density, which can be regarded as a sign of the partial chiral symmetry restoration. When the value of c_1 is decreased, the corresponding value of G becomes larger (see Fig. 1) to reproduce the nucleon mass.

	UV	IR
X	0	$\sigma_0 z_m^3/2$
V_0	μ	-
$\partial_z V_0$	-	0
N_1	0	c_2
N_2	0	$c_2 * c_1$

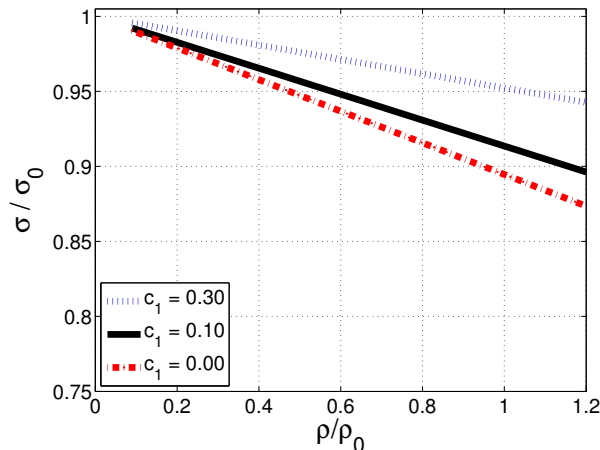Table 2: Boundary condition at finite density. The mark "-" indicates that the value is not fixed.

Figure 4: Density dependence of σ/σ_0 for several choices of c_1.

Since the larger G implies the larger correction to the scalar from the nucleon matter, the smaller c_1 we choose, the more rapidly the condensate σ decreases. The degreasing property of the chiral condensate is similar to the one obtained in Ref. [1].

We next show the resultant equation of state, a relation between the chemical potential and the baryon number density in Fig. 5. This figure shows that the chemical potential increases with the increasing baryon number density. This does not agree with the nature, in which the chemical potential decreases against the density in the low density region below the normal nuclear matter density. This decreasing property is achieved by the subtle cancellation between the repulsive and attractive forces. So this increasing property indicates that, in the present model, the repulsive force mediated by the U(1) gauge field is stronger than the attractive force mediated by the scalar degree included in X field.

For studying the attractive force mediated by the scalar fields, we extract the density dependence of the effective nucleon mass using the Walecka type model (see e.g. Refs. [6;7]), in which the chemical potential μ is expressed as

$$\mu = \sum_{n=1}^{\infty} \frac{g_{\omega^{(n)}NN}^2}{m_{\omega^{(n)}}^2} \rho_b + \sqrt{k_F^2 + M^{*2}} \, , \tag{14}$$

where ρ_b is the baryon number density, $g_{\omega^{(n)}NN}$ is the coupling for nth eigenstate of the omega mesons, $m_{\omega^{(n)}}$ is its mass, k_F is the Fermi momentum, and M^* is the effective nucleon mass. Note that, in the free Fermi gas, k_F is related to ρ_b as $\rho_b = \frac{2k_F^3}{3\pi^2}$, which leads to $k_F = \left(\frac{3\pi^2\rho_b}{2}\right)^{1/3}$. In the present hQCD model, the $\omega^{(n)}NN$ coupling is calculated in vacuum as $g_{\omega^{(n)}NN} = 15.5 \sim 15.8, 8.9 \sim 10.9\ldots$ depending on the value of c_1. Using these couplings together with the masses of $m_{\omega^{(n)}} \sim 780, 1794 \ldots$ MeV, we convert the density dependence of μ obtained above into the one of
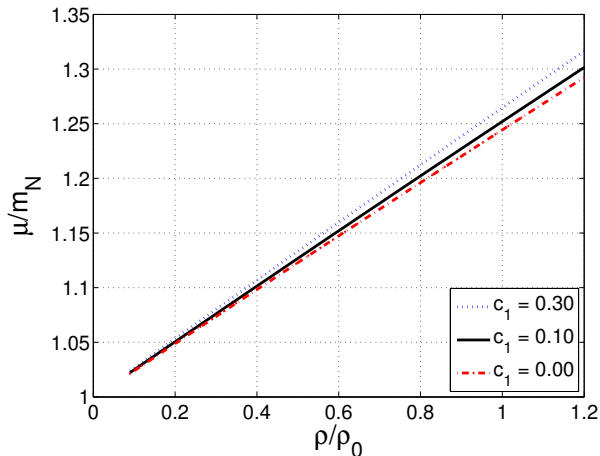
Figure 5: Equation of state. The horizontal axis shows the baryon number density normalized by the normal nuclear matter density of $\rho_0 = 0.16\,(\mathrm{fm})^{-3}$, and the vertical axis does the chemical potential by the nucleon mass of $0.94\,\mathrm{GeV}$. The dashed line shows the EoS for $c_1 = 0$, the solid line for $c_1 = 0.1$ and the dotted line for $c_1 = 0.3$.

the effective nucleon mass M^* through Eq. (14). We plot the density dependence of the effective mass M^* in Fig. 6. This shows that the effective mass decreases with increasing density. The decreasing
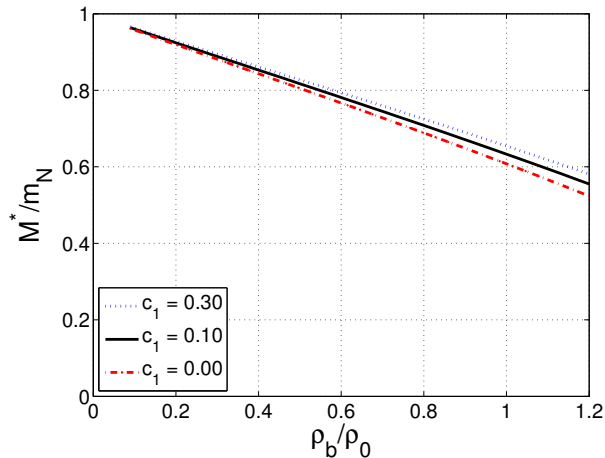

Figure 6: Density dependence of the effective nucleon mass M^*.

rate is larger than the one obtained in Ref. [1], which is the reflection of the iterative corrections included through the holographic mean field theory. It should be noted that the decreasing of M^* is more rapid for smaller value of c_1. In other word, the larger the percentage of the mass coming from the chiral symmetry breaking is, more rapidly the effective mass M^* decreases with density.

4   A summary and discussions

We develop the holographic mean field approach in a bottom-up holographic QCD model proposed in Ref. [3] which includes five-dimensional baryon field in the model proposed in Refs. [4;5].

In the present analysis, we made an analysis only at the mean field level. So a natural extension

is to consider the fluctuations on the top of the mean field obtained here. It is also interesting to study the relation between the isospin chemical potential and the isospin density based on the approach developed in this paper, since the relation has a relevance to the symmetry energy. We leave these works to the future project.

References

[1] Y. Kim, C. -H. Lee and H. -U. Yee, Phys. Rev. D **77**, 085030 (2008) [arXiv:0707.2637 [hep-ph]]; K-I. Kim, S. H. Lee and Y. Kim, in *proceedings of Workshop on Hadron and Nuclear Physics, HNP09, Osaka, Japan, 2009* (World Scientific, Hackensack, 2010).

[2] M. Harada, S. Nakamura and S. Takemoto, Phys. Rev. D **86**, 021901 (2012) [arXiv:1112.2114 [hep-th]].

[3] D. K. Hong, T. Inami, and H.-U. Yee, Phys.Lett. **B646**,

[4] J. Erlich, E. Katz, D. T. Son, and M. A. Stephanov, Phys.Rev.Lett. **95**,

[5] L. Da Rold and A. Pomarol, Nucl.Phys. **B721**,

[6] J. Walecka, Annals Phys. **83**, 491 (1974).

[7] T. Matsui, Nucl.Phys. **A370**, 365 (1981).

[8] B. R. He and M. Harada, [arXiv:1304.7866].